Lattice Polarons across the Superfluid to Mott Insulator Transition

V. E. Colussi,[1,*] F. Caleffi,[2] C. Menotti,[1] and A. Recati[1,3]
[1]Pitaevskii BEC Center, CNR-INO and Dipartimento di Fisica, Università di Trento, I-38123 Trento, Italy
[2]International School for Advanced Studies (SISSA), Via Bonomea 265, I-34136 Trieste, Italy
[3]Trento Institute for Fundamental Physics and Applications, INFN, Via Sommarive 14, 38123 Povo, Trento, Italy

(Received 20 May 2022; revised 11 January 2023; accepted 17 March 2023; published 27 April 2023)

We study the physics of a mobile impurity confined in a two-dimensional lattice, moving within a Bose-Hubbard bath at zero temperature. Exploiting the quantum Gutzwiller formalism, we develop a beyond-Fröhlich model of the bath-impurity interaction to describe the properties of the polaronic quasiparticle formed by the dressing of the impurity by quantum fluctuations of the bath. We find a stable and well-defined polaron throughout the entire phase diagram of the bath, except for the very low tunneling limit of the hard-core superfluid. The polaron properties are highly sensitive to the different universality classes of the quantum phase transition between the superfluid and Mott insulating phases, providing an unambiguous probe of correlations and collective modes in a quantum critical many-body environment.

DOI: 10.1103/PhysRevLett.130.173002

Introduction.—Polarons, quasiparticles formed by a mobile impurity dressed by a cloud of excitations of the bath in which they are immersed, are ubiquitous in physics. Important examples include quantum materials [1], superfluid helium [2], nuclear matter [3], and ultracold atomic gases [4]. Crucially, an ultracold atomic bath is clean, and its equation of state and the bath-impurity coupling are highly controllable [5,6], enabling recent pioneering measurements of polaronic quasiparticle properties [7–11]. Moreover, ultracold atoms have provided new platforms for quantum simulation [12,13], in particular using optical lattices to realize Hubbard models [14,15], prominent in the study of strongly correlated materials. In these lattice many-body systems, particularly in quantum critical regimes of the bath, understanding the role played by polarons and quantum fluctuations in determining exotic properties such as high-temperature superconductivity is of fundamental importance [16–31].

Studies of impurities in quantum critical baths, beyond addressing the fundamental polaron properties, yield valuable insights also into the role of impurities as probes of nontrivial quantum and thermal correlations in their environment. In continuous systems, this may include the discontinuity of the energy of a polaron across the Berezinskii-Kosterlitz-Thouless transition [32] and the disappearance of the Bose polaron across the transition for Bose-Einstein condensation [33].

Bose polarons in lattices were first considered for a continuous Bose-Einstein condensed bath [34,35]. A qualitatively new feature arises in a Bose-Hubbard (BH) environment, namely that the bath undergoes a superfluid (SF) to Mott insulator (MI) phase transition at strong interactions and integer filling. This transition, and its distinct universality classes [36–38] [see Fig. 1(a)], drastically change the quantum correlations and excitations of the environment and should therefore significantly affect the properties of the Bose lattice polaron. So far, the BH bath has been addressed only in the deep MI or SF regimes where mean-field theory applies [39–41]. The effects of quantum criticality are still largely unexplored, having been examined so far only theoretically for fixed impurities [37].

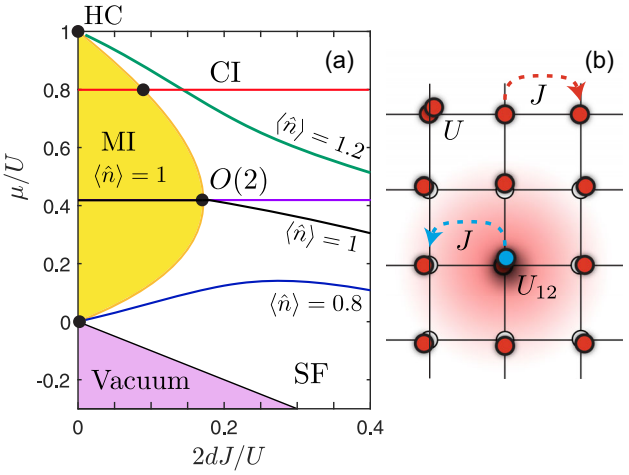

FIG. 1. (a) Mean-field Gutzwiller phase diagram of a Bose-Hubbard bath on a d-dimensional lattice around the $\langle\hat{n}\rangle = 1$ MI lobe showing constant $\langle\hat{n}\rangle$ (blue, black, green) and μ/U (red, blue) lines. The SF to MI transition can be crossed at the tip at constant integer density ($O(2)$) transition or on the edges via the commensurate-incommensurate (CI) transition. For increasing interaction strength U, noninteger filling lines connect deep and hard-core (HC) regimes of the superfluid. (b) A mobile impurity with hopping J and coupling U_{12} to a BH bath is dressed by a cloud of excitations, producing a Bose lattice polaron.

In this Letter, we study the fundamental properties of Bose lattice polarons throughout the entire phase diagram of a BH bath. Thanks to the recent development of the Quantum Gutzwiller (QGW) method [37,42–44], the effects of quantum fluctuations in a BH system on a *mobile* impurity can now be systematically included. In particular, we develop a powerful procedure for expanding bath-impurity interactions in terms of elementary excitations. We show that in the quantum critical and insulating regimes this expansion must include terms *beyond* the celebrated Fröhlich model for polarons in crystals [45]. The many-band structure of the elementary excitations and nonlinear effects are shown to be crucial in capturing the effect of the universality classes of the SF to MI transition on the Bose lattice polaron. Across the SF to MI transition, we find nonmonotonic and nonanalytic polaron properties. In the strongly interacting SF regime, divergences occur since the mobile impurity becomes orthogonal to its bare state due to a very large density response of the bath.

Method.—We consider a mobile impurity coupled to a two-dimensional ($d = 2$) bosonic bath, both confined to a uniform square lattice. The impurity and the surrounding cloud of excited bath modes produce the polaronic quasiparticle illustrated in Fig. 1(b). The properties of the polaron are determined by the self-energy $\Sigma(\boldsymbol{k},\omega) = G^{(0)}(\boldsymbol{k},\omega)^{-1} - G(\boldsymbol{k},\omega)^{-1}$, where $G^{(0)}(\boldsymbol{k},\omega)[G(\boldsymbol{k},\omega)]$ is the bare (interacting) impurity Green's function. We calculate the polaron energy dispersion by ignoring the imaginary part of the self-energy. The full polaron energy $E_{\boldsymbol{k}} = \varepsilon_{\boldsymbol{k}} + \mathrm{Re}\Sigma(\boldsymbol{k}, E_{\boldsymbol{k}})$, where $\varepsilon_{\boldsymbol{k}}$ is the energy dispersion of a free impurity, can be expanded at low momentum as

$$E_{\boldsymbol{k}} = E_0 + \frac{\boldsymbol{k}^2}{2M_*} + O(k^4), \tag{1}$$

where E_0 is the bath-induced shift of the polaron energy, M_* is the polaron effective mass, and we have set $\hbar = 1$. The coherence and stability of the polaron are given by the momentum-dependent quasiparticle residue and decay rate

$$Z_{\boldsymbol{k}}^{-1} = 1 - \left.\frac{\partial \mathrm{Re}\Sigma(\boldsymbol{k},\omega)}{\partial\omega}\right|_{\omega=E_{\boldsymbol{k}}}, \qquad \Gamma_{\boldsymbol{k}} = -2Z_{\boldsymbol{k}}\mathrm{Im}\Sigma(\boldsymbol{k}, E_{\boldsymbol{k}}), \tag{2}$$

respectively. The quasiparticle residue measures the overlap between the polaron and free impurity states, quantifying the renormalized spectral weight of the polaronic pole in the interacting Green's function [46]. The polaron is a well-defined quasiparticle provided that $\Gamma_{\boldsymbol{k}} \ll E_{\boldsymbol{k}}$ and $Z_{\boldsymbol{k}}$ is nonzero.

In our treatment, we assume weak impurity-bath on-site couplings U_{12}, such that the impurity and bath energy scales are well-separated. In this regime, the back action of the impurity on the zero-temperature bath ground state can be neglected and the bath remains stable in the presence of the impurity.

Model.—The microscopic model is $\hat{H} = \hat{H}_B + \hat{H}_I + \hat{H}_{IB}$, where

$$\hat{H}_B = -J\sum_{\langle \boldsymbol{r},\boldsymbol{s}\rangle}(\hat{a}_{\boldsymbol{r}}^\dagger \hat{a}_{\boldsymbol{s}} + \mathrm{H.c.}) + \frac{U}{2}\sum_{\boldsymbol{r}}\hat{a}_{\boldsymbol{r}}^\dagger\hat{a}_{\boldsymbol{r}}^\dagger\hat{a}_{\boldsymbol{r}}\hat{a}_{\boldsymbol{r}} - \mu\sum_{\boldsymbol{r}}\hat{n}_{\boldsymbol{r}},$$
$$\hat{H}_I = \sum_{\boldsymbol{k}}\varepsilon_{\boldsymbol{k}}\hat{a}_{I,\boldsymbol{k}}^\dagger\hat{a}_{I,\boldsymbol{k}}, \qquad \hat{H}_{IB} = U_{12}\sum_{\boldsymbol{r}}\hat{n}_{\boldsymbol{r}}\hat{n}_{I,\boldsymbol{r}}, \tag{3}$$

are the Hamiltonians describing the bath, the impurity, and the bath-impurity coupling, respectively. The lattice is composed by I sites with lattice spacing set to unity without loss of generality [47]. The bosonic operators $\hat{a}_{\boldsymbol{r}}^\dagger$ and $\hat{a}_{\boldsymbol{r}}$ create and destroy, respectively, a bath particle at lattice site $\boldsymbol{r}$ and are related to the local density operator as $\hat{n}_{\boldsymbol{r}} = \hat{a}_{\boldsymbol{r}}^\dagger\hat{a}_{\boldsymbol{r}}$. Here, $\varepsilon_{\boldsymbol{k}} = 4J\sum_{i=1}^2 \sin^2(k_i/2)$ is the energy dispersion of a free impurity on a uniform lattice, $\hat{a}_{I,\boldsymbol{k}}^\dagger$ ($\hat{a}_{I,\boldsymbol{k}}$) and $\hat{n}_{I,\boldsymbol{r}} = \hat{a}_{I,\boldsymbol{r}}^\dagger\hat{a}_{I,\boldsymbol{r}}$ are respectively the creation (destruction) and local density operators of the impurity, while U (μ) is the on-site interaction strength (chemical potential) of the bath. For simplicity, we assume that the bath and impurity hopping parameters J between neighboring sites $\langle \boldsymbol{r},\boldsymbol{s}\rangle$ are equal, setting their "bare" effective masses $M^{-1} = 2J$.

The ground state of the BH bath can be approximated by the Gutzwiller wave function $|\Psi_G\rangle = \otimes_{\boldsymbol{r}}\sum_n c_n^0|n,\boldsymbol{r}\rangle$ [48–50], yielding the phase diagram in Fig. 1(a). Fluctuations on top of this mean-field state can be characterized using the QGW method [42–44]. Within this approach, the quantized fluctuations correspond to the elementary many-body excitations of the system $\delta\hat{c}_n(\boldsymbol{r}) = I^{-1/2}\sum_{\alpha\boldsymbol{k}} e^{i\boldsymbol{k}\cdot\boldsymbol{r}}(u_{\alpha,\boldsymbol{k},n}\hat{b}_{\alpha,\boldsymbol{k}} + v_{\alpha,\boldsymbol{k},n}\hat{b}_{\alpha,-\boldsymbol{k}}^\dagger)$. Keeping terms up to quadratic order in the fluctuations, we diagonalize the bath Hamiltonian $\hat{H}_B \approx \sum_{\alpha,\boldsymbol{k}}\omega_{\alpha,\boldsymbol{k}}\hat{b}_{\alpha,\boldsymbol{k}}^\dagger\hat{b}_{\alpha,\boldsymbol{k}}$ in analogy with the number conserving Bogoliubov theory of weakly interacting gases [51,52]. Here, $\hat{b}_{\alpha,\boldsymbol{k}}(\hat{b}_{\alpha,\boldsymbol{k}}^\dagger)$ represents the annihilation (creation) of a single collective mode in the αth branch with momentum $\boldsymbol{k}$ and energy $\omega_{\alpha,\boldsymbol{k}}$. The QGW method improves upon the Bogoliubov description, which is valid only in the weakly interacting SF regime [34,35,39,41]. It has been proven to provide a robust treatment of both local and nonlocal quantum correlation in BH models, even in critical regimes where quantum fluctuations are strong [43,44].

We recall briefly that the excitation spectrum of the BH bath differs significantly from the continuous case and presents a multibranch structure. The two energetically lowest excitations in the SF regime consist of the gapless Goldstone and gapped amplitude (Higgs) modes, which in the MI phase become gapped particle and hole excitations [52,60–63]. At the tip of the MI lobe, both Goldstone and Higgs modes are gapless, and the bath filling is integer and equal on both sides of an $O(2)$ transition (c.f. Ref. [60]). On the lobe boundary away from the tip, the Goldstone mode

becomes quadratic whereas the Higgs mode remains gapped. Consequently, the system behaves as an effective free Bose gas of quasiparticles despite being strongly interacting [60]. Away from the tip, the density undergoes an abrupt change and for this reason is often referred to as the commensurate-incommensurate (CI) transition. Crucially, the QGW model is able to essentially capture both universality classes of the SF to MI quantum phase transition as shown in Refs. [43,52].

We take into account the multibranch spectrum of bath excitations forming the polaron cloud by expanding $\hat{H}_{IB}$ in powers of the $\hat{b}_{\alpha,k}$ and $\hat{b}^{\dagger}_{\alpha,k}$ [52], and find

$$\hat{H}_{IB} \approx U_{12}\sum_{r}\hat{n}_{I,r}[n_0 + \delta_1\hat{n}(\boldsymbol{r}) + \delta_2\hat{n}(\boldsymbol{r}) + \ldots]. \quad (4)$$

The first term in the above expansion is the mean-field energy shift $U_{12}n_0$, where $n_0 = \sum_n n|c_n^0|^2$ is the mean-field bath density, while the second term reads

$$\delta_1\hat{n}(\boldsymbol{r}) = \frac{1}{\sqrt{I}}\sum_{\alpha}\sum_{\boldsymbol{k}} N_{\alpha,\boldsymbol{k}}(\hat{b}_{\alpha,\boldsymbol{k}}e^{i\boldsymbol{k}\cdot\boldsymbol{r}} + \hat{b}^{\dagger}_{\alpha,\boldsymbol{k}}e^{-i\boldsymbol{k}\cdot\boldsymbol{r}}), \quad (5)$$

with $N_{\alpha,\boldsymbol{k}} = \sum_n nc_n^0(u_{\alpha,\boldsymbol{k},n} + v_{\alpha,\boldsymbol{k},n})$. Already at this level, thanks to the inclusion of the multibranch excitations, the resultant Fröhlich model [45,46] is more general than the usual Bogoliubov expansion on top of a SF state [39,64,65], accurate only in the weakly interacting deep SF regime [52]. However, since two-particle processes play a crucial role in the MI and quantum critical regimes [37], it is necessary to include also the nonlinear term

$$\delta_2\hat{n}(\boldsymbol{r}) = \frac{1}{I}\sum_{\alpha,\beta}\sum_{\boldsymbol{k},p}[W_{\alpha\boldsymbol{k},\beta\boldsymbol{p}}(\hat{b}^{\dagger}_{\alpha,\boldsymbol{k}}\hat{b}^{\dagger}_{\beta,\boldsymbol{p}}e^{-i(\boldsymbol{k}+\boldsymbol{p})\cdot\boldsymbol{r}} + \text{H.c.}) + U_{\alpha\boldsymbol{k},\beta\boldsymbol{p}}\hat{b}^{\dagger}_{\alpha,\boldsymbol{k}}\hat{b}_{\beta,\boldsymbol{p}}e^{i(\boldsymbol{p}-\boldsymbol{k})\cdot\boldsymbol{r}} + V_{\alpha\boldsymbol{k},\beta\boldsymbol{p}}\hat{b}_{\alpha,\boldsymbol{k}}\hat{b}^{\dagger}_{\beta,\boldsymbol{p}}e^{i(\boldsymbol{k}-\boldsymbol{p})\cdot\boldsymbol{r}}], \quad (6)$$

which leads to a *beyond*-Fröhlich model of the bath-impurity interaction. At zero temperature, which is the case under consideration in this Letter, only the two-particle terms $W_{\alpha\boldsymbol{k},\beta\boldsymbol{p}} = \sum_n(n-n_0)u_{\alpha,\boldsymbol{k},n}v_{\beta,\boldsymbol{p},n}$ contribute [52].

Self-energy.—We calculate the self-energy diagrammatically via the Dyson series, including all relevant zero-temperature diagrams to second order in U_{12} shown in Fig. 2. This level of approximation amounts to the replacement $E_{\boldsymbol{k}} \to \varepsilon_{\boldsymbol{k}}$ in evaluating Eqs. (1) and (2). Within the QGW approach, we find

$$\Sigma(\boldsymbol{k},\omega) = U_{12}\langle\hat{n}\rangle + \frac{U_{12}^2}{I}\sum_{\alpha}\sum_{\boldsymbol{q}}\frac{|N_{\alpha,\boldsymbol{q}}|^2}{\omega - \omega_{\alpha,\boldsymbol{q}} - \varepsilon_{\boldsymbol{k}-\boldsymbol{q}} + i0^+} + \frac{U_{12}^2}{2I^2}\sum_{\alpha,\beta}\sum_{\boldsymbol{q},\boldsymbol{q}'}\frac{|W_{\alpha\boldsymbol{q},\beta\boldsymbol{q}'} + W_{\beta\boldsymbol{q}',\alpha\boldsymbol{q}}|^2}{\omega - \omega_{\alpha,\boldsymbol{q}} - \omega_{\beta,\boldsymbol{q}'} - \varepsilon_{\boldsymbol{k}-\boldsymbol{q}-\boldsymbol{q}'} + i0^+}, \quad (7)$$

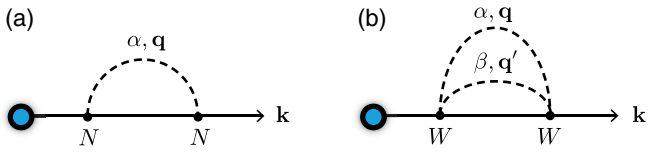

FIG. 2. Diagrammatic representation of the beyond mean-field contributions to the interacting impurity Green's function to second order in U_{12} within the zero-temperature QGW approach. (a) and (b) depict the one- and two-particle diagrams with QGW vertex functions $N_{\alpha,\boldsymbol{q}}$ and $W_{\alpha\boldsymbol{q},\beta\boldsymbol{q}'}$, respectively. Full lines represent the bare impurity Green's function $G^{(0)}$, while dashed lines correspond to bare Green's functions $D_{\alpha}^{(0)}$ of the collective modes of the BH bath.

with the one-particle vertex $N_{\alpha,\boldsymbol{k}}$ [Fig. 2(a)], two-particle direct $W_{\alpha\boldsymbol{k},\beta\boldsymbol{k}'}$, and exchange $W_{\beta\boldsymbol{k}',\alpha\boldsymbol{k}}$ vertices [Fig. 2(b)], and the Hartree shift $U_{12}\langle\hat{n}\rangle$ where $\langle\hat{n}\rangle = n_0 + \langle\delta_2\hat{n}\rangle$ is the quantum-corrected bath density.

Importantly, *both* one- and two-particle processes contribute at order $(U_{12}/U)^2$ in Eq. (7). This allows for a nontrivial description of the Bose lattice polaron in a MI bath, where the only available excitations are particle-hole pairs and also accounts for competing one- and two-particle processes in the SF phase, as discussed below.

In the remainder of this Letter, the properties of the Bose lattice polaron are discussed throughout the entire phase diagram of the BH bath with emphasis on how they are affected by the SF to MI transition and its different universality classes. Results are given in units of $\eta \equiv (U_{12}/U)^2$.

Spectral properties.—We analyze first the results for the spectral properties E_0 and M/M_* obtained by evaluating Eq. (1) and shown in Figs. 3(a)–3(d) [52]. Upon crossing the $O(2)$ phase transition, either via fixed filling or chemical potential, we see that both E_0 and M/M_* reach an absolute minimum on the SF side and increase *smoothly* across the transition. As a result of the closing of the Higgs gap at this critical point [52], the weight of one- and two-particle processes becomes comparable due to the absorption and emission of Goldstone-Higgs pairs by the mobile impurity.

The situation changes drastically when the MI boundary is crossed instead at the CI transition, as shown in Figs. 3(a) and 3(c) for fixed chemical potential. As this transition is crossed for progressively smaller J/U, due to the decreasing sound velocity associated with the Goldstone mode, the bath becomes softer to perturbations of the density by the mobile impurity [43,49]. This physics is dominated by one-particle processes involving the Goldstone mode, as the Higgs mode remains gapped. This stronger bath-impurity interplay yields sharper, nonanalytic polaron properties across the phase boundary [Fig. 3(c) inset], which closely reflect the discontinuous behavior of the one-body coherence length [43,60].

Moving at constant noninteger filling, the bath remains always in the SF phase, in spite of becoming strongly

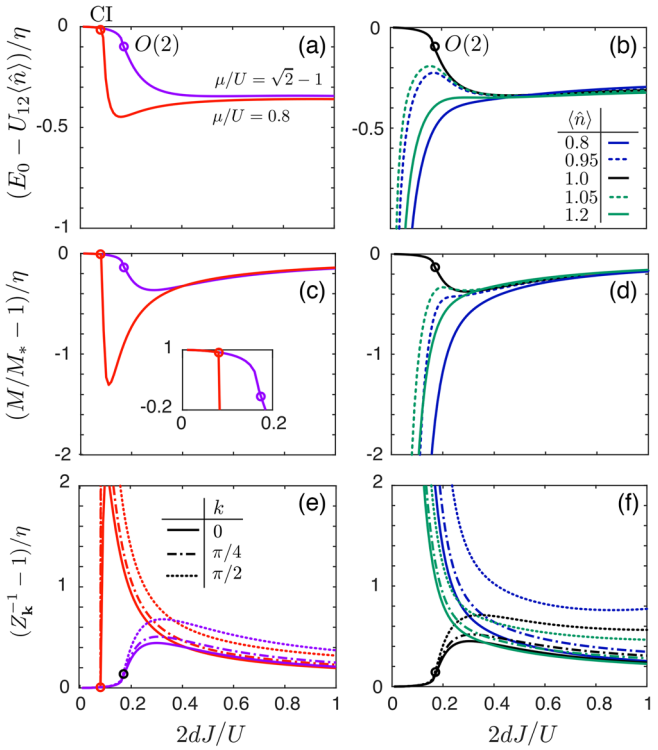

FIG. 3. (a),(c),(e) Polaron properties for fixed μ/U across the $O(2)$ (blue) and CI (red) transitions, with the nonanalytical nature of the latter shown in the inset of panel (c). (b),(d),(f) Polaron properties at (black) integer and (green, blue) noninteger filling of the bath $\langle\hat{n}\rangle$. Dots indicate the quantum critical points shown in Fig. 1.

interacting, and enters the hard-core (HC) SF state for $J/U \to 0$ indicated in Fig. 1(a). In the HC SF regime, the polaron cloud is again dominated by one-particle processes involving only the Goldstone mode with a vanishingly small sound speed and therefore a substantially quadratic, rather than linear, dispersion. This amounts to a free Bose gas of strongly renormalized quasiparticles. The infinite compressibility of the HC SF leads to a dramatic interplay between density fluctuations of the bath and the impurity as shown in Figs. 3(b) and 3(d). The results for E_0 and M/M_* closely follow the $O(2)$ line up to J/U slightly larger than the tip of the lobe, after which the bath enters the strongly interacting SF regime and divergences take over. This gives rise to an overall nonmonotonic behavior [dotted lines Figs. 3(b) and 3(d)].

Coherence and stability properties.—The quantum critical nature of the bath can also strongly influence the coherence (Z_k) and stability (Γ_k) of the polaron, jeopardizing its experimental detection. In Figs. 3(e) and 3(f), we present our numerical results for Z_k. Across the $O(2)$ transition, the polaron remains coherent ($Z_k > 1 - \eta$) at all momenta whereas its coherence rapidly deteriorates across the CI transition at finite momentum. In general, the coherence of the polaron in the SF regime worsens as the bath becomes increasingly strongly interacting. Eventually, the residue even vanishes in the limiting case of the HC SF regime as shown in Fig. 3(f). Here, the mobile impurity becomes orthogonal to its bare state, giving rise to a bosonic instance of Anderson's orthogonality catastrophe [66]. Whereas this effect occurs in a free Bose gas in the continuum, in the BH model it occurs in the strongly interacting regime of the bath, highlighting the unusual behavior of the HC SF as an effectively free Bose gas of quasiparticles. In both cases the infinite compressibility of the bath generates a macroscopic polaron cloud [67–70]. Additionally, the coherence of the polaron in the HC SF regime is predicted to spoil over time [37] even for static impurities, while the mobile impurity is expected to follow a quantum Brownian motion [71].

To analyze the decay rate Γ_k, we use Eq. (2) to derive an analytical expression that is reminiscent of the Landau criterion for superfluidity [5,52,70],

$$\Gamma_k \approx \theta(k - k_c)\frac{4U_{12}^2\kappa}{3\pi}\sqrt{2k_c}(k - k_c)^{3/2}, \tag{8}$$

where κ is the bath compressibility [49], and θ is the Heaviside step function. This result applies at small impurity momentum in the thermodynamic limit of the SF regime where the one-particle spontaneous emission of a phonon mode dominates. Energy conservation for this process sets a critical value for the impurity momentum $k_c = Mc_s$, where c_s is the sound velocity associated with the Goldstone mode. A similar result has been obtained within the Bogoliubov approach for a mobile impurity in a continuous Bose bath [70,72].

The behavior of both κ and c_s in the quantum critical regimes of the BH bath differs significantly from the continuous case. Namely, as the SF to MI transition is crossed for progressively smaller J/U, the bath becomes increasingly compressible while the sound speed tends to vanish. This yields nontrivial critical momentum k_c and decay rate Γ_k as shown in Fig. 4. We find that in general the polaron is long-lived in the incompressible MI phase. The

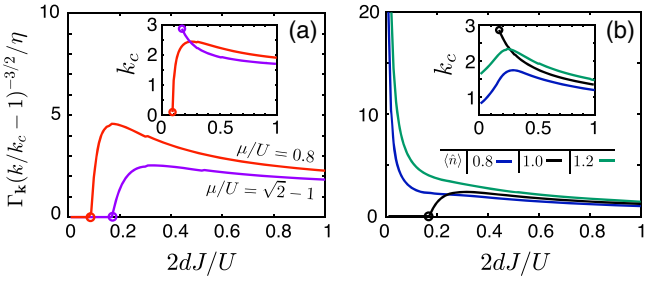

FIG. 4. Behavior of the polaron decay rate [see Eq. (8)] for (a) fixed μ/U across the $O(2)$ (blue) and CI (red) transitions; (b) fixed $\langle\hat{n}\rangle$ at integer filling (black) across the $O(2)$ transition and noninteger fillings (blue, green). Dots indicate quantum critical points, with the Landau-critical values of the impurity momentum k_c shown in the insets.

decay rate reaches instead a maximum when approaching the $O(2)$ and CI transitions, with the behavior of k_c depending strongly on the universality class [Fig. 4 insets]. In the HC SF, the bath is highly compressible; however the critical momentum k_c remains finite, resulting in a divergence of the decay rate $\Gamma_{\boldsymbol{k}}$. This mirrors the divergence of E_0 in Fig. 3(b) and the orthogonality catastrophe in Fig. 3(f), indicating that (i) the polaron is no longer a well-defined quasiparticle, and (ii) the potential for macroscopic deformation of the bath by the impurity cannot be neglected. Consequently the assumptions underlying our Letter are violated. A complete treatment of these subtle effects requires a self-consistent calculation, which is possible within the two-component Gutzwiller approach [73–75] recently developed in Ref. [44]. This analysis is, however, beyond the scope of this Letter.

Conclusion.—By blending diagrammatic techniques with the recently developed quantum Gutzwiller method, we have studied the fundamental quasiparticle properties of the Bose lattice polaron, i.e., of an impurity embedded in a BH bath, and highlighted the role of the bath SF to MI transition and its different universality classes. In the MI and $O(2)$ critical regimes, we have shown that processes beyond the celebrated Fröhlich model for polarons must be taken into account. These processes involve the creation and annihilation of pairs of elementary excitations belonging to the multibranch spectrum of the BH bath. We find nonmonotonic polaron properties across the SF to MI phase transition, namely a maximum of the effective mass and a minimum of the residue close to the lobe tips. A stronger and sharper renormalization of the polaron properties is found when crossing the transition at noninteger fillings, due to the large compressibility of the strongly correlated superfluid in the low-tunneling regime. For the same reason, the polaron properties show a diverging behavior for fixed noninteger filling and increasing bath interaction strengths, approaching the hard-core superfluid regime. Consequently, studies of this regime, which is ill-defined within our approach, should account for the modification of the bath in the presence of the impurity.

Our analysis, which has been carried out to second order in the bath-impurity interaction, shows that the polaron persists as a well-defined quasiparticle in most regimes of the BH bath. Stronger bath-impurity interactions can be accounted for using ladder approximations (c.f. [76]); however, we expect that the behaviors found in this Letter will not change qualitatively.

We thank Georg M. Bruun, Ragheed Alhyder, and Stefano Giorgini for fruitful discussions and constructive feedback. This project has received financial support from Provincia Autonoma di Trento and the Italian MIUR through the PRIN2017 project CEnTraL (Protocol No. 20172H2SC4).

*Corresponding author.
colussiv@gmail.com

[1] C. Franchini, M. Reticcioli, M. Setvin, and U. Diebold, Nat. Rev. Mater. **6**, 560 (2021).
[2] J. Bardeen, G. Baym, and D. Pines, Phys. Rev. **156**, 207 (1967).
[3] M. Kutschera and W. Wójcik, Phys. Rev. C **47**, 1077 (1993).
[4] F. Scazza, M. Zaccanti, P. Massignan, M. M. Parish, and J. Levinsen, Atoms **10**, 22 (2022).
[5] L. Pitaevskii and S. Stringari, *Bose-Einstein Condensation and Superfluidity* (Oxford University Press, Oxford, 2016), Vol. 164.
[6] C. Chin, R. Grimm, P. Julienne, and E. Tiesinga, Rev. Mod. Phys. **82**, 1225 (2010).
[7] A. Schirotzek, C.-H. Wu, A. Sommer, and M. W. Zwierlein, Phys. Rev. Lett. **102**, 230402 (2009).
[8] S. Nascimbène, N. Navon, K. J. Jiang, L. Tarruell, M. Teichmann, J. McKeever, F. Chevy, and C. Salomon, Phys. Rev. Lett. **103**, 170402 (2009).
[9] M.-G. Hu, M. J. Van de Graaff, D. Kedar, J. P. Corson, E. A. Cornell, and D. S. Jin, Phys. Rev. Lett. **117**, 055301 (2016).
[10] N. B. Jørgensen, L. Wacker, K. T. Skalmstang, M. M. Parish, J. Levinsen, R. S. Christensen, G. M. Bruun, and J. J. Arlt, Phys. Rev. Lett. **117**, 055302 (2016).
[11] F. Scazza, G. Valtolina, P. Massignan, A. Recati, A. Amico, A. Burchianti, C. Fort, M. Inguscio, M. Zaccanti, and G. Roati, Phys. Rev. Lett. **118**, 083602 (2017).
[12] I. Bloch, J. Dalibard, and S. Nascimbène, Nat. Phys. **8**, 267 (2012).
[13] I. M. Georgescu, S. Ashhab, and F. Nori, Rev. Mod. Phys. **86**, 153 (2014).
[14] D. Jaksch, C. Bruder, J. I. Cirac, C. W. Gardiner, and P. Zoller, Phys. Rev. Lett. **81**, 3108 (1998).
[15] C. Gross and I. Bloch, Science **357**, 995 (2017).
[16] P. A. Lee, N. Nagaosa, and X.-G. Wen, Rev. Mod. Phys. **78**, 17 (2006).
[17] A. S. Alexandrov and N. F. Mott, Rep. Prog. Phys. **57**, 1197 (1994).
[18] A. S. Alexandrov, Phys. Rev. B **77**, 094502 (2008).
[19] J. P. F. LeBlanc *et al.* (Simons Collaboration on the Many-Electron Problem), Phys. Rev. X **5**, 041041 (2015).
[20] V. J. Emery, Phys. Rev. Lett. **58**, 2794 (1987).
[21] E. Dagotto, Rev. Mod. Phys. **66**, 763 (1994).
[22] J. R. Schrieffer, X.-G. Wen, and S.-C. Zhang, Phys. Rev. Lett. **60**, 944 (1988).
[23] Z. Liu and E. Manousakis, Phys. Rev. B **44**, 2414 (1991).
[24] G. Martinez and P. Horsch, Phys. Rev. B **44**, 317 (1991).
[25] S. Sachdev, Phys. Rev. B **39**, 12232 (1989).
[26] E. Dagotto, A. Moreo, and T. Barnes, Phys. Rev. B **40**, 6721 (1989).
[27] C. L. Kane, P. A. Lee, and N. Read, Phys. Rev. B **39**, 6880 (1989).
[28] B. I. Shraiman and E. D. Siggia, Phys. Rev. Lett. **61**, 467 (1988).
[29] S. Schmitt-Rink, C. M. Varma, and A. E. Ruckenstein, Phys. Rev. Lett. **60**, 2793 (1988).
[30] F. Grusdt, M. Kánasz-Nagy, A. Bohrdt, C. S. Chiu, G. Ji, M. Greiner, D. Greif, and E. Demler, Phys. Rev. X **8**, 011046 (2018).

[31] K. K. Nielsen, M. A. Bastarrachea-Magnani, T. Pohl, and G. M. Bruun, Phys. Rev. B **104**, 155136 (2021).
[32] R. Alhyder and G. M. Bruun, Phys. Rev. A **105**, 063303 (2022).
[33] Z. Z. Yan, Y. Ni, C. Robens, and M. W. Zwierlein, Science **368**, 190 (2020).
[34] M. Bruderer, A. Klein, S. R. Clark, and D. Jaksch, Phys. Rev. A **76**, 011605(R) (2007).
[35] F. Grusdt, A. Shashi, D. Abanin, and E. Demler, Phys. Rev. A **90**, 063610 (2014).
[36] M. Greiner, O. Mandel, T. Esslinger, T. W. Hänsch, and I. Bloch, Nature (London) **415**, 39 (2002).
[37] F. Caleffi, M. Capone, I. de Vega, and A. Recati, New J. Phys. **23**, 033018 (2021).
[38] D. Rossini, T. Calarco, V. Giovannetti, S. Montangero, and R. Fazio, Phys. Rev. A **75**, 032333 (2007).
[39] D. Benjamin and E. Demler, Phys. Rev. A **89**, 033615 (2014).
[40] Y. Kato, K. A. Al-Hassanieh, A. E. Feiguin, E. Timmermans, and C. D. Batista, Europhys. Lett. **98**, 46003 (2012).
[41] S. Dutta and E. J. Mueller, Phys. Rev. A **88**, 053601 (2013).
[42] F. Caleffi, Quantum fluctuations beyond the Gutzwiller approximation in the Bose-Hubbard model, Master's thesis, University of Trento, 2018.
[43] F. Caleffi, M. Capone, C. Menotti, I. Carusotto, and A. Recati, Phys. Rev. Res. **2**, 033276 (2020).
[44] V. E. Colussi, F. Caleffi, C. Menotti, and A. Recati, SciPost Phys. **12**, 111 (2022).
[45] H. Fröhlich, Adv. Phys. **3**, 325 (1954).
[46] G. D. Mahan, *Many-Particle Physics* (Springer Science & Business Media, New York, 2013).
[47] Analytic expressions are written for a d-dimensional lattice to emphasize the generality of the QGW approach.
[48] W. Krauth, M. Caffarel, and J.-P. Bouchaud, Phys. Rev. B **45**, 3137 (1992).
[49] K. V. Krutitsky and P. Navez, Phys. Rev. A **84**, 033602 (2011).
[50] K. V. Krutitsky, Phys. Rep. **607**, 1 (2016).
[51] Y. Castin, *Lecture Notes of Les Houches Summer School*, édité par C. W. R. Kaiser and F. David (Springer-Verlag, Berlin/Heidelberg, 2001).
[52] See Supplemental Material at http://link.aps.org/supplemental/10.1103/PhysRevLett.130.173002 for details of our model and calculations, which includes Refs. [53–59].
[53] F. Grusdt and E. Demler, *Quantum Matter at Ultralow Temperatures* (2015), Vol. 191, pp. 325–411.
[54] D. S. Rokhsar and B. G. Kotliar, Phys. Rev. B **44**, 10328 (1991).
[55] K. Sheshadri, H. R. Krishnamurthy, R. Pandit, and T. V. Ramakrishnan, Europhys. Lett. **22**, 257 (1993).
[56] C. Cohen-Tannoudji, J. Dupont-Roc, and G. Grynberg, *Photons and Atoms: Introduction to Quantum Electrodynamics* (Wiley-VCH Verlag GmbH & Co. KGaA, Weinheim, Germany, 1997).
[57] J.-P. Blaizot and G. Ripka, *Quantum Theory of Finite Systems* (MIT Press, Cambridge, Massachusetts, 1985).
[58] F. Grusdt, G. E. Astrakharchik, and E. Demler, New J. Phys. **19**, 103035 (2017).
[59] F. Grusdt, K. Seetharam, Y. Shchadilova, and E. Demler, Phys. Rev. A **97**, 033612 (2018).
[60] S. Sachdev, *Quantum Phase Transitions*, 2nd ed. (Cambridge University Press, Cambridge, England, 2011).
[61] M. Di Liberto, A. Recati, N. Trivedi, I. Carusotto, and C. Menotti, Phys. Rev. Lett. **120**, 073201 (2018).
[62] S. D. Huber, E. Altman, H. P. Büchler, and G. Blatter, Phys. Rev. B **75**, 085106 (2007).
[63] M. Endres, T. Fukuhara, D. Pekker, M. Cheneau, P. Schauß, C. Gross, E. Demler, S. Kuhr, and I. Bloch, Nature (London) **487**, 454 (2012).
[64] A. M. Rey, K. Burnett, R. Roth, M. Edwards, C. J. Williams, and C. W. Clark, J. Phys. B **36**, 825 (2003).
[65] F. Cosco, M. Borrelli, J. J. Mendoza-Arenas, F. Plastina, D. Jaksch, and S. Maniscalco, Phys. Rev. A **97**, 040101(R) (2018).
[66] P. W. Anderson, Phys. Rev. Lett. **18**, 1049 (1967).
[67] N.-E. Guenther, R. Schmidt, G. M. Bruun, V. Gurarie, and P. Massignan, Phys. Rev. A **103**, 013317 (2021).
[68] S. M. Yoshida, S. Endo, J. Levinsen, and M. M. Parish, Phys. Rev. X **8**, 011024 (2018).
[69] J. Sun, O. Rambow, and Q. Si, arXiv:cond-mat/0404590.
[70] A. Novikov and M. Ovchinnikov, J. Phys. A **42**, 135301 (2009).
[71] A. Lampo, S. H. Lim, M. Á. García-March, and M. Lewenstein, Quantum **1**, 30 (2017).
[72] G. E. Astrakharchik and L. P. Pitaevskii, Phys. Rev. A **70**, 013608 (2004).
[73] P. Buonsante, S. M. Giampaolo, F. Illuminati, V. Penna, and A. Vezzani, Phys. Rev. Lett. **100**, 240402 (2008).
[74] T. Ozaki, I. Danshita, and T. Nikuni, arXiv:1210.1370.
[75] B. Capogrosso-Sansone, M. Guglielmino, and V. Penna, Laser Phys. **21**, 1443 (2011).
[76] N.-E. Guenther, P. Massignan, M. Lewenstein, and G. M. Bruun, Phys. Rev. Lett. **120**, 050405 (2018).